Development of a Hypoxia-Selective Near-Infrared Fluorescent Probe for Non-invasive Tumor Imaging

Bahaa Gamal Mohamed Youssif,[a,b] Kensuke Okuda,[a] Tetsuya Kadonosono,[c] Ola Ibrahim Abdel Razek Salem,[b] Alaa Arafat Mohamed Hayallah,[b] Mostafa Ahmed Hussein,[b] Shinae Kizaka-Kondoh,[c] and Hideko Nagasawa*,[a]

[a] *Laboratory of Medicinal and Pharmaceutical Chemistry, Gifu Pharmaceutical University; Gifu 501–1196, Japan:* [b] *Pharmaceutical Organic Chemistry Department, Faculty of Pharmacy, Assiut University; Assiut 71526, Egypt: and* [c] *Division of Biofunctional Engineering, School of Bioscience and Biotechnology, Tokyo Institute of Technology; Midori-ku, Yokohama 226–8503, Japan.* Received September 30, 2011; accepted December 31, 2011

A near-infrared fluorochrome, GPU-311, was designed, synthesized and evaluated for its application in non-invasive imaging of tumor hypoxia. Efficient synthesis was achieved by nucleophilic substitution and click chemistry ring using the bifunctional tetraethylene glycol linker 2 containing thiol and azide groups for the conjugation of the propargylated nitroimidazole 1 and the heptamethine cyanine dye 3 bearing a 2-chloro-1-cyclohexenyl ring. GPU-311 exhibited long excitation and emission wavelength (Ex/Em=785/802 nm) and a decent quantum yield (0.05). The water solubility and hydrophilicity of GPU-311 increased. After *in vitro* treatment of SUIT-2/HRE-Luc pancreatic cancer cells with GPU-311, a higher level of fluorescence was observed selectively in hypoxia than in normoxia. However, *in vivo* fluorescence imaging of a mouse xenograft model after GPU-311 administration revealed inadequate accumulation of GPU-311 in tumors due to its rapid elimination through the liver.

Key words near-infrared fluorescence; tumor hypoxia; 2-nitroimidazole; *in vivo* imaging

Tumor hypoxia is now known as one of the most prominent features of malignant neoplasias, distinguishing them from normal tissues.[1)] The hypoxic status of various solid tumors can markedly influence the therapeutic response of malignant tumors to conventional irradiation, chemotherapy and other nonsurgical treatment modalities.[2,3)] Therefore, there has been a growing impetus to develop non-invasive imaging methods to detect and assess tumor hypoxia.[4,5)]

In the development of imaging probes for tumor hypoxia, nitroimidazoles have received particular attention as exogenous markers because of their unique behavior in hypoxic environments owing to their high electron affinity.[4)] Nitroimidazole compounds undergo selective bioreduction in hypoxic cells to form reactive species that irreversibly bind to cellular macromolecules.[6)] Currently, positron emission tomography using nitroimidazole tracers is the most advanced technique to achieve non-invasive *in vivo* mapping of tumor hypoxia with anatomical resolution.[7)] However, radionuclide imaging requires radioactive compounds which have an intrinsically limited half-life and expose the patient and practitioner to ionizing radiation, and are therefore subject to a variety of stringent safety regulations that limit their repeated use.

In contrast, optical imaging has comparable sensitivity to radionuclide imaging, and it can be "targeted" if the emitting fluorophore is conjugated to a targeting ligand.[8)] That is safer and easier to perform than nuclear imaging. Optical imaging in the near-infrared (NIR) region (700—900 nm) has a low absorption by intrinsic photoactive biomolecules and allows light to penetrate several centimeters into the tissue, a depth sufficient for imaging practically all small animal models.[9)] Therefore, NIR fluorescence imaging, a less expensive and non-invasive technique, may be a powerful tool for imaging tumor hypoxia. Recently, we developed an NIR hypoxia probe, GPU-167 (Fig. 1), comprising 2-nitroimidazole and tricarbocyanine dye, for *in vivo* imaging of tumor hypoxia.[10)] This is the first chemical probe to visualize tumor hypoxia by NIR fluorescence with significant tumor-to-background (T/B) ratio in a mouse xenograft model. GPU-167 maintained a good T/B ratio (>2.5), and it was retained for a relatively longer period (>48 h) in the body. However, the considerably high liver distribution of GPU-167 was similar to that observed in the tumor. In this study, to improve the pharmacokinetic properties and synthetic yield of GPU-167, we designed and synthesized a new NIR fluorescent probe, GPU-311 for *in vivo* imaging of tumor hypoxia.

As shown in Fig. 2, the molecular design involved conjugation of a 2-nitroimidazole derivative as a hypoxia marker and a heptamethine cyanine dye as an NIR fluorescent dye through a polyether linker. To synthesize GPU-311, we employed the chloro-substituted heptamethine cyanine dye **3**[11)] as an intermediate fluorophore, which has a 2-chloro-1-cyclohexenyl ring moiety providing a chemical reactive site for nucleophilic substitution at the center methine carbon and increased photostability in comparison to cyanine dyes with an open polymethine chain.[12)] Thus we can easily connect a hypoxia target moiety to the fluorophore through a suitable linker. In addition, GPU-311 has two sulfonate groups which

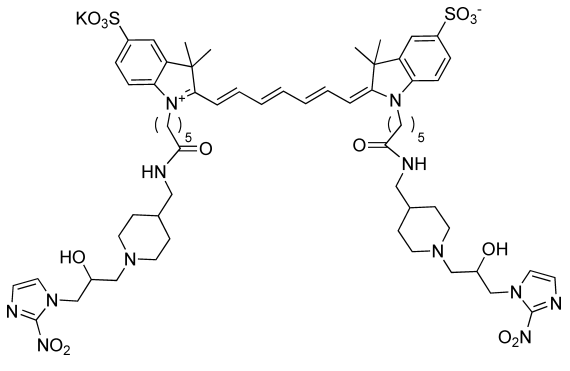

Fig. 1. Structure of GPU-167

* To whom correspondence should be addressed. e-mail: hnagasawa@gifu-pu.ac.jp

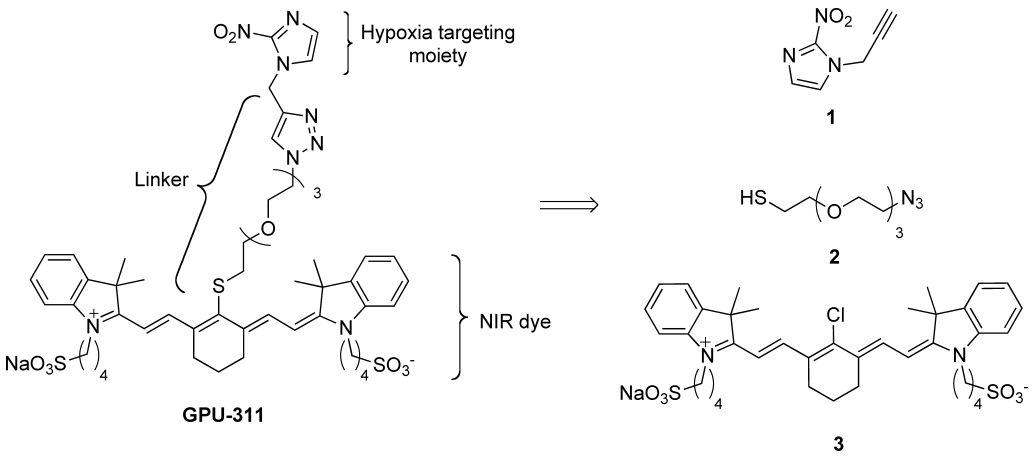

Fig. 2. Molecular Design of GPU-311

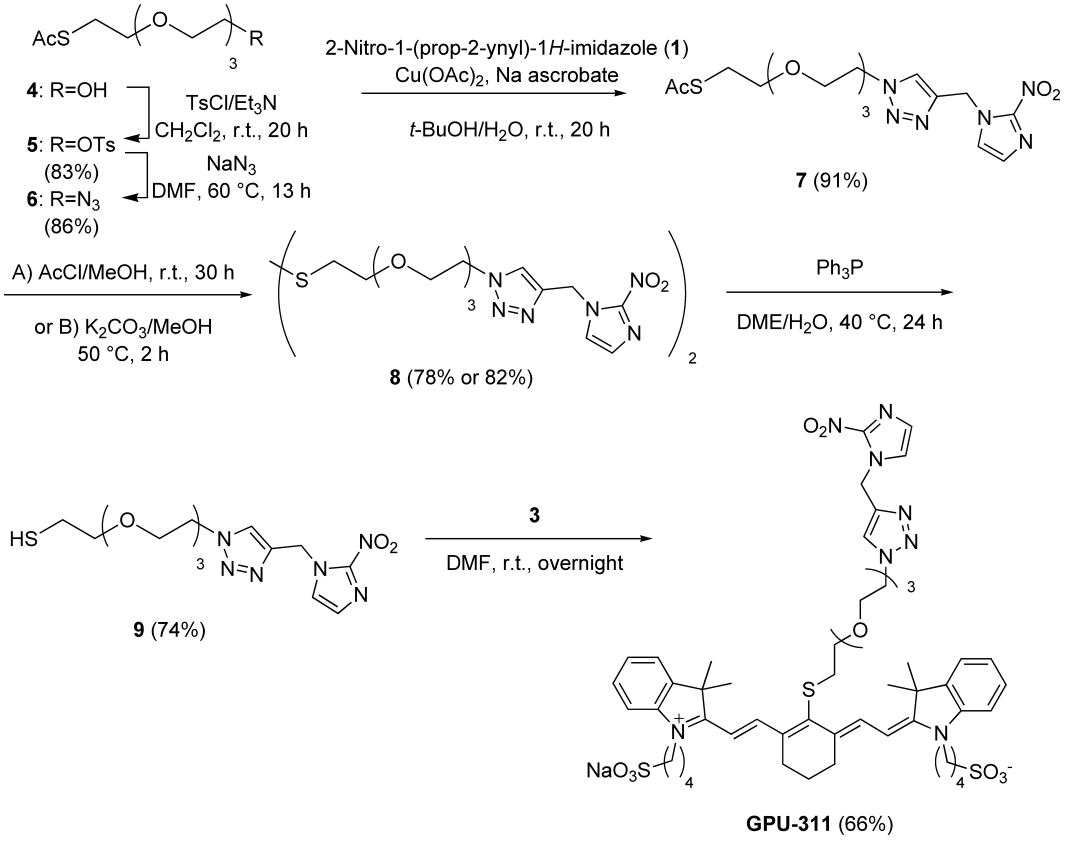

Chart 1. Synthesis of Hypoxia Probe, GPU-311

increase water solubility and prevent dye aggregation.[13] Then, the bifunctional tetraethylene glycol linker **2** containing thiol and azide groups was employed to increase the hydrophilicity of the probe compared to GPU-167 and to facilitate crosslinking between the NIR dye and 2-nitroimidazole moiety.[14] A triazole linker was selected owing to its metabolic stability and ease of introduction from azide- and alkyne-functionalized precursors using click chemistry.[15] Good nucleophilicity of thiol is suitable for substitution at the central vinylogous halide carbon of the chloro-substituted dye **3** to connect the linker moiety, and the triazole-forming click reaction is a reliable method to link molecules; thus we designed GPU-311 as a probe candidate (Fig. 2). Propargylated nitroimidazole **1**,[16] linker **2**, and NIR dye **3** are the key intermediates for developing the probe.

Compounds **1** and **3** were prepared according to the procedure mentioned in previous studies.[11,16] Then compound **9**, which consisted of **1** and **2**, was prepared from the known *S*-11-hydroxy-3,6,9-trioxaundecyl ethanethioate (**4**)[17] in six steps (Chart 1). First, tosylation of **4** followed by azide substitution gave **6**[14] (71% yield, two steps), and then a Cu(I)-catalyzed 1,3-dipolar cycloaddition reaction with **1** yielded **7** at a 91% yield. An attempt to deprotect the acetyl group of **7** caused accompanying disulfide formation of the product by either acid (method A) or alkaline treatment (method B) to produce **8** (78% or 82% yield, respectively). Reduction of

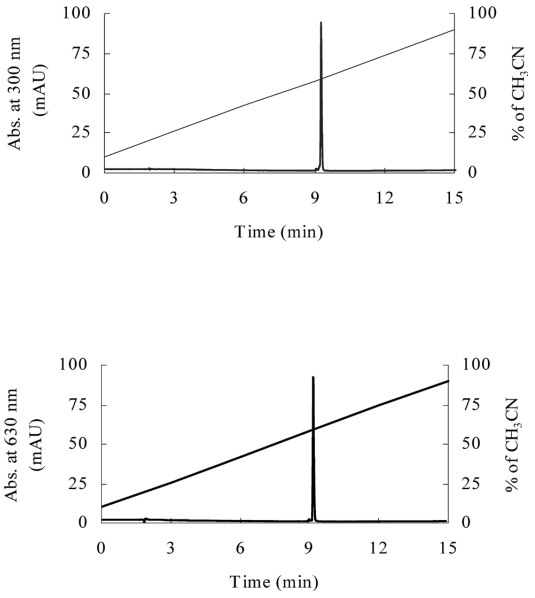

Fig. 3. LC Spectra of GPU-311

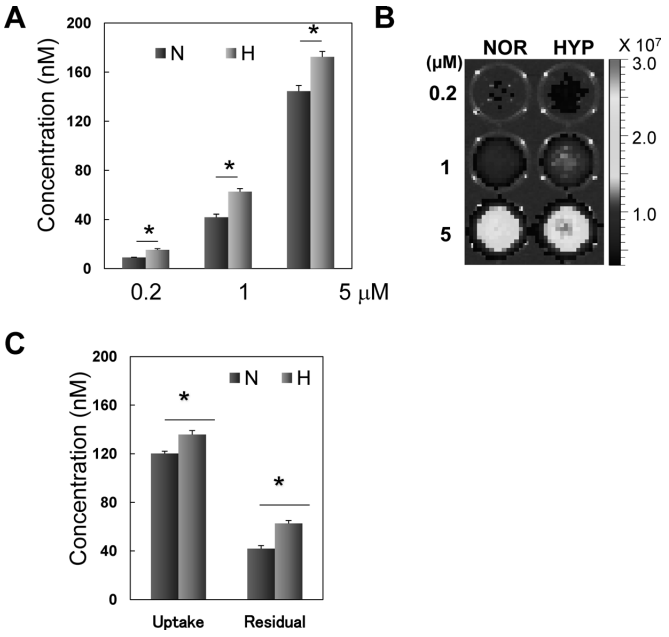

Fig. 4. (A) Accumulation of GPU-311 to Hypoxic Cells *in Vitro*, (B) Representative Fluorescence Image, (C) Cellular Uptake of GPU-311

(A) The SUIT-2/HRE-Luc cells (2×10^5 cells) cultured under normoxic (N) or hypoxic (H) conditions were treated with GPU-311 and analyzed by measurement of fluorescent intensity with an Ex/Em wavelength of 740 nm/780 nm (*$p<0.05$, $n=3$). The amount of GPU-311 in the cells was calculated by using intensity–concentration curve. (B) NIR imaging was performed using an IVIS spectrum (Ex/Em=710 nm/800 nm), (C) Cellular uptake was evaluated from fluorescent intensity immediately after the probe treatment at the concentration of 1 μM, while intracellular residual binding was examined after the probe treatment and post-incubation in fresh medium for 1 h.

8 by triphenylphosphine produced **9** (74% yield). Finally, the target molecule GPU-311 was obtained in 66% yield by the reaction of **3** with excess amount of **9**. It was purified by C18 reversed-phase flash chromatography. Purity and identity were determined by NMR and LC-MS, which yielded single peaks at both 300 nm and 630 nm absorption (Fig. 3) and a high-resolution mass spectrum with *m/z* 1077.4260 for $C_{52}H_{69}N_8O_{11}S_3$ ($[M-Na+2H]^+$). The evaluation of the photophysical properties of GPU-311 revealed the absorption and emission peaks at 785 and 802 nm, respectively, a large extinction coefficient ($1.2\times10^4\,M^{-1}cm^{-1}$ at 785 nm) and a decent quantum yield (0.05). The hydrophobicity index (Rm) of GPU-311 and GPU-167 was examined by a reversed-phase thin-layer chromatographic system (mobile phase: 10% 5 mM sodium phosphate buffer, pH 7.4 and 90% methanol). GPU-311 was believed to be more hydrophilic than GPU-167 due to their Rm values (−0.43 *vs.* −0.26).

To evaluate the hypoxia selectivity of GPU-311, an *in vitro* fluorescence assay was performed using SUIT-2/HRE-Luc pancreatic cancer cells.[18] In the assay, after treatment with GPU-311 under normoxic or hypoxic conditions for 30 min, the cells were incubated for 1 h in fresh medium under normoxic condition and washed with phosphate buffered saline (PBS) to remove unbound dye. During post-incubation in fresh medium, unbound probe should be released outside the cells. We compared intensity of cellular fluorescence of GPU-311 treated in hypoxic or aerobic condition before or after post-incubation, to distinguish between nonspecific cellular uptake and irreversible intracellular binding. When the cells were cultured in hypoxia (0.1% O_2) and normoxia (21% O_2) with GPU-311 at concentrations of 0.2, 1 and 5 μM, and then exposed to post-incubation for 1 h in fresh medium, significantly stronger fluorescence signals were detected by probe treatment in hypoxia than in normoxia (Figs. 4A, B). As shown in Fig. 4C, fluorescence signals of hypoxic cells were higher than that of normoxic cells even before post-incubation. After post-incubation, fluorescence signals of hypoxic cells decreased by half, while those of aerobic cells decreased by one third. These results suggested that GPU-311 may penetrate and bind to intracellular substances irreversibly in hypoxic cells significantly more than in aerobic cells.

Next, GPU-311 was evaluated by *in vivo* experiments using xenografts of SUIT-2/HRE-Luc cells according to the procedure described in previous studies.[19] The SUIT-2/HRE-Luc cells stably carry 5HRE-luciferase, a luciferase reporter gene under the control of the hypoxia-inducible factor (HIF)-dependent promoter, and thus HIF-1-activity in xenografts can be monitored by bioluminescence imaging. When GPU-311 was injected into tumor-bearing mice, GPU-311 could reveal the tumors 3 h after injection with the highest T/B ratio of 2.52 (Fig. 5). In SUIT-2/HRE-Luc cells, HIF-1α expression is undetectable under normoxic conditions but significantly increased under hypoxic conditions because HIF-1α stability is strictly regulated by oxygen concentration.[18] Then, to confirm the existence of hypoxic tumor cells, bioluminescence emitted from HIF-1-active hypoxic cells was also examined 24 h after injection of GPU-311 (Fig. 5A, right panel). Fluorescence signals of GPU-311 were observed in the forefoot and the abdominal regions after 3 h (Fig. 5A, left panel). The signal in the forefoot seemed to be correlated with the bioluminescent signal of the tumor, suggesting that the fluorescence owing to GPU-311 in the tumor was related to hypoxia. However, fluorescence signals of GPU-311 in the tumor rapidly disappeared 6 h after its injection, suggesting that the fluorescence signal of GPU-311 was unstable in hypoxic tumors. The fluorescence signal of GPU-311 was also detected in the abdominal region until 24 h. In comparison with GPU-167, the clearance of GPU-311 became much faster, while tumor accumulation was

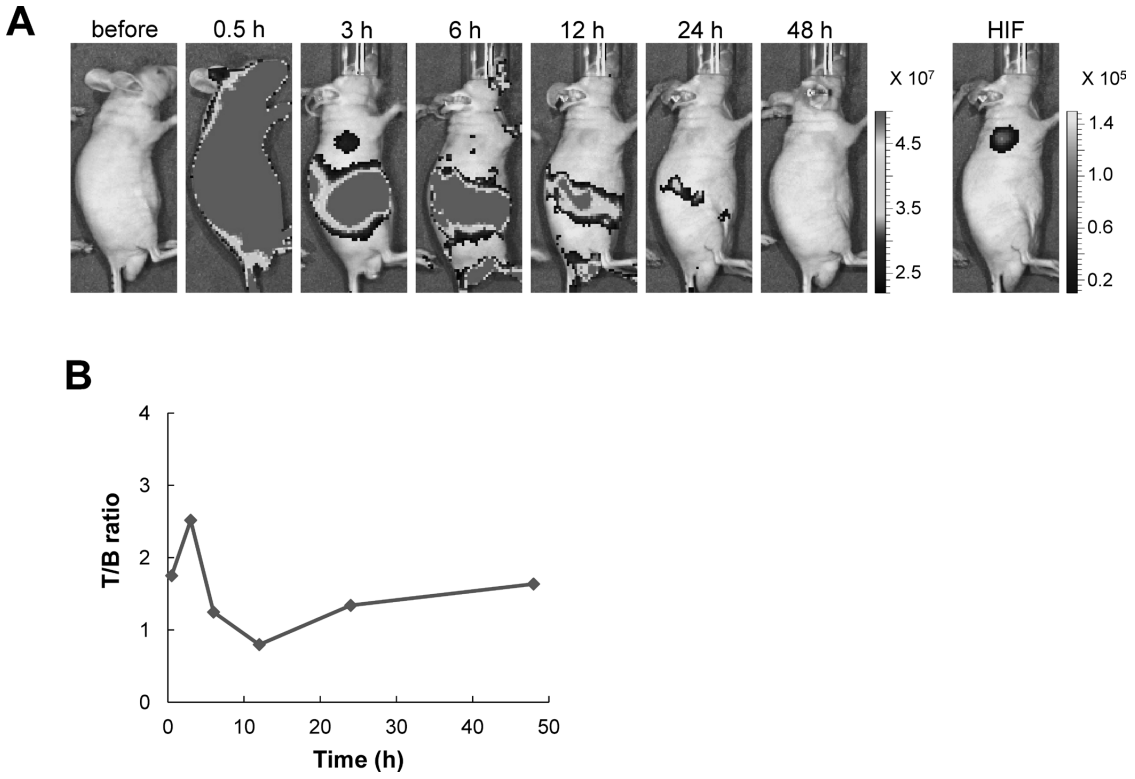

Fig. 5. (A) *In Vivo* Optical Imaging of Hypoxic Region in Subcutaneous Cancers with GPU-311, (B) The Relative Fluorescence Intensity of the Tumor to the Muscle (T/B Ratio)

(A) Representative *in vivo* image of hypoxic tumors after 10 nmol of GPU-311 administration. Nude mouse carrying SUIT-2/HRE-Luc xenografts in both forefeet were imaged at the indicated time after GPU-311 injection. The right panel (HIF) shows bioluminescent image of HIF-1-active hypoxic tumor at 24 h. The minimum and maximum photons/s/cm^2/steradian of each image was indicated in each figure by a color bar scale. (B) Fluorescence intensities of the SUIT-2/HRE-Luc xenografts and the muscle of the hind foot were measured at the indicated time after GPU-311 administration.

declined significantly. These data suggest that the hypoxia probe requires further optimization of the hydrophilic–hydrophobic balance.

In summary, we developed an NIR fluorescent hypoxia probe, GPU-311, which was synthesized using simple procedures to produce moderate or good yields and was easily purified. It exhibited good optical properties, high hydrophilicity and significant *in vitro* hypoxia selectivity. According to *in vivo* imaging, although GPU-311 was obviously detected with an adequate T/B ratio (2.52) in tumors 3 h after injection, its fluorescence intensity was not strong, and most of the probe was thought to be rapidly eliminated though the liver due to its considerable hydrophilicity. Consequently, the design strategy of nitroimidazole–NIR cyanine dye conjugates appears promising for developing hypoxia probes for *in vivo* tumor imaging. However, further molecular modifications are necessary to improve the pharmacokinetics of the nitroimidazole–NIR dye conjugates to be applicable for *in vivo* hypoxia imaging.

Experimental

General Information Unless otherwise stated, all reagents and solvents were obtained from Sigma-Aldrich, Wako (Japan), Nacalai (Japan), or TCI without further purification. Normal-phase TLC was carried out on Silica gel 60 F_{254} (Merck, 1.05715.0009) using reagent graded solvents. Normal-phase column chromatography was performed on silica gel (AP-300, Dai koh Trading Co., Ltd.). Reverse-phase TLC was performed on RP-18 F_{254S} (Merck, 1.15389). All moisture or air-sensitive reactions were carried out under nitrogen atmosphere. ^{1}H-NMR spectra were obtained with JEOL JNM-ECA500 spectrometer at 500 MHz frequency or JNM-AL400 spectrometer at 400 MHz frequency in $CDCl_3$ or DMSO-d_6 with tetramethylsilane as an internal standard. Chemical shifts are reported in ppm. Coupling constants are reported in Hz. The multiplicity is defined by s (singlet), d (doublet), t (triplet), dd (doublet of doublets), br (broad), and m (multiplet). The direct analysis in real time (DART)-MS measurements were carried out on a JEOL JMS-T100TD. The electrospray ionization (ESI)-MS measurements were carried out on a Shimadzu LCMS-IT-time-of-flight (TOF). UV-Vis spectra were obtained by Beckman DU-600 spectrophotometer. The fluorescence excitation spectra and emission spectra were obtained by JASCO FP-6600 Fluorescence spectrophotometer. The slit width was 5 nm for excitation and 10 nm for emission. 2-Nitro-1-(prop-2-ynyl)-1*H*-imidazole (**1**),[16] tricarobycyanine dye **3**,[11] *S*-11-hydroxy-3,6,9-trioxaundecyl ethanethioate (**4**)[17] were prepared according to the literature procedures.

***S*-11-(Tosyloxy)-3,6,9-trioxaundecyl Ethanethioate (5)** To an ice-cooled solution of **4**[17] (500 mg, 2.0 mmol) in CH_2Cl_2 (5 mL), *p*-toluene sulfonyl chloride (TsCl) (570 mg, 3.0 mmol) in CH_2Cl_2 (2 mL) and triethylamine (400 mg, 4.0 mmol) were added. The mixture was stirred at room temperature for 20 h. Water (5 mL) was added to the mixture, and then extracted with $CHCl_3$ (3×10 mL). The organic phase was washed with water and brine, dried over anhydrous Na_2SO_4 and concentrated. The crude product was purified by column chromatography using diethyl ether as an eluent to give **5** (670 mg, 83%) as a yellow oil. ^{1}H-NMR ($CDCl_3$, 500 MHz) δ: 2.32 (3H, s), 2.44

(3H, s), 3.07 (2H, t, J=6.6 Hz), 3.56—3.59 (6H, m), 3.59 (4H, s), 3.68 (2H, t, J=4.7 Hz), 4.16 (2H, t, J=4.8 Hz), 7.35 (2H, d, J=8.2 Hz), 7.79 (2H, d, J=8.3 Hz). High resolution (HR)-DART-MS m/z: 407.1195 ($[M+H]^+$, Calcd for $C_{17}H_{27}O_7S_2$: 407.1198).

***S*-11-Azido-3,6,9-trioxaundecyl Ethanethioate (6)**[14] To a solution of **5** (600 mg, 1.5 mmol) in dry *N*,*N*-dimethylformamide (DMF) (10 mL), sodium azide (480 mg, 7.4 mmol) was added. The reaction mixture was heated at 60°C while stirring for 13 h. After the solvent was removed, the residue was poured into water and extracted with CH_2Cl_2 (3×10 mL). The organic phase was washed with water and brine, dried over anhydrous Na_2SO_4, filtered and concentrated. the crude product was purified by column chromatography using $CHCl_3$–methanol (95 : 5, v/v) as an eluent to afford **6** as yellow oil; yield (350 mg, 86%). ^{1}H-NMR ($CDCl_3$, 500 MHz) δ: 2.34 (3H, s), 3.10 (2H, t, J=6.6 Hz), 3.40 (2H, t, J=5.1 Hz), 3.61 (2H, t, J=6.4 Hz), 3.62–3.67 (4H, m), 3.67 (4H, s), 3.69 (2H, t, J=4.8 Hz). HR-DART-MS m/z: 278.1174 ($[M+H]^+$, Calcd for $C_{10}H_{20}N_3O_4S$: 278.1175).

***S*-11-{4-[(2-Nitro-1*H*-imidazol-1-yl)methyl]-1*H*-1,2,3-triazol-1-yl}-3,6,9-trioxaundecyl Ethanethioate (7)** To a solution of **1**[16] (200 mg, 1.3 mmol) in a mixture of *tert*-butanol–H_2O (1 : 1 (v/v), 5 mL), **6** (440 mg, 1.6 mmol), copper(II) acetate (24 mg, 0.13 mmol) and sodium ascorbate (52 mg, 0.26 mmol) were added. The resulting mixture was stirred at room temperature for 20 h, and the residue was extracted with $CHCl_3$ (3×10 mL). The organic phase was washed with water, dried over anhydrous Na_2SO_4 and concentrated. The crude product was purified by column chromatography using $CHCl_3$–methanol (19 : 1, v/v) as an eluent to give **7** (515 mg, 91%) as a waxy solid. ^{1}H-NMR ($CDCl_3$, 500 MHz): δ: 2.32 (3H, s), 3.07 (2H, t, J=6.5 Hz), 3.59 (2H, t, J=6.6 Hz), 3.61 (4H, s), 3.62 (4H, s), 3.87 (2H, t, J=5.0 Hz), 4.56 (2H, t, J=4.9 Hz), 5.72 (2H, s), 7.14 (1H, d, J=1.1 Hz), 7.39 (1H, d, J=1.2 Hz), 7.95 (1H, s). HR-DART-MS m/z: 429.1550 ($[M+H]^+$, Calcd for $C_{16}H_{25}N_6O_6S$: 429.1556).

Bis(11-{4-[(2-nitro-1*H*-imidazol-1-yl)methyl]-1*H*-1,2,3-triazol-1-yl}-3,6,9-trioxaundecan-1-yl) Disulfide (8) To a solution of **7** (240 mg, 0.56 mmol) in methanol (3 mL), acetyl chloride (0.57 mL, 8.0 mmol) was added. The resulting mixture was stirred at room temperature for 30 h, CH_2Cl_2 and H_2O (5 mL each) was added to the mixture. A saturated $NaHCO_3$ solution was added until pH 7. The organic layer was washed with water (5 mL) and concentrated. The obtained crude product was purified by column chromatography using $CHCl_3$–methanol (9 : 1, v/v) as an eluent to give **8** as a light yellow waxy solid (168 mg, 78%). ^{1}H-NMR ($CDCl_3$, 500 MHz) δ: 2.86 (4H, t, J=6.5 Hz), 3.60 (8H, s), 3.62 (8H, s), 3.71 (4H, t, J=6.5 Hz), 3.86 (4H, t, J=5.0 Hz), 4.55 (4H, t, J=4.9 Hz), 5.71 (4H, s), 7.125 (1H, s), 7.127 (1H, s), 7.386 (1H, s), 7.388 (1H, s), 7.95 (2H, s).

The another procedure was as follows. To a solution of **7** (100 mg, 0.23 mmol) in dry methanol (2 mL), K_2CO_3 (120 mg, 0.87 mmol) was added. The resulting mixture was stirred at 50°C for 2 h. A saturated solution of NH_4Cl (5 mL) was added and the mixture was extracted with EtOAc (3×10 mL). The organic phase was washed with water, dried over anhydrous Na_2SO_4 and concentrated. The obtained crude product was purified by column chromatography using $CHCl_3$–methanol (9 : 1, v/v) as an eluent to give **8** as waxy solid; yield (74 mg, 82%). The spectroscopic data was identical to the product by acid hydrolysis described above.

11-{4-[(2-Nitro-1*H*-imidazol-1-yl)methyl]-1*H*-1,2,3-triazol-1-yl}-3,6,9-trioxaundecan-1-thiol (9) To a solution of **8** (100 mg, 0.13 mmol) in a mixture of dimethoxyethane–H_2O (2 : 1 (v/v), 9 mL), triphenyl phosphine (40 mg, 0.15 mmol) was added. The resulting mixture was stirred at 40°C for 24 h. The mixture was extracted with $CHCl_3$ (3×10 mL), the organic phase was washed with water, dried over anhydrous $MgSO_4$ and concentrated. The crude product was purified by column chromatography using $CHCl_3$–methanol (9 : 1, v/v) as an eluent to give **9** (74 mg, 74%) as a waxy solid. ^{1}H-NMR ($CDCl_3$, 500 MHz) δ: 1.60 (1H, t, J=8.1 Hz, D_2O exchangeable), 2.68 (2H, q, J=6.9 Hz), 3.62 (6H, s), 3.63 (4H, s), 3.87 (2H, t, J=4.9 Hz), 4.55 (2H, t, J=5.0 Hz), 5.72 (2H, s), 7.14 (1H, s), 7.39 (1H, s), 7.94 (1H, s). HR-DART-MS m/z: 387.1464 ($[M+H]^+$, Calcd for $C_{14}H_{23}N_6O_5S$: 387.1451).

Tricarbocyanine GPU-311 To a solution of **3** (35 mg, 0.047 mmol) in DMF (4 mL), **9** (60 mg, 0.16 mmol) was added. The mixture was stirred for 18 h at room temperature. After the solvent was removed, the residue was dissolved in methanol (2 mL) and then precipitated by diethyl ether (25 mL). The solid was filtered and further purified by Yamazen flash liquid chromatography W-Prep 2XY system equipped with Ultra Pack ODS-SM-50B column (26 mm inner diameter×300 mm length) using 0.1 M triethylammonium acetate buffer (pH 7.3)/acetonitrile (30–60% in 70 min) as an eluent to give GPU-311 (34 mg, 66%) as a dark green solid. ^{1}H-NMR (DMSO-d_6, 400 MHz) δ: 1.69 (12H, s), 1.77—1.80 (10H, m), 2.54 (4H, t, J=7.1 Hz), 2.66 (4H, br), 2.97 (2H, t, J=6.1 Hz), 3.44 (6H, br), 3.46 (2H, t, J=5.1 Hz), 3.56 (2H, t, J=6.2 Hz), 3.76 (2H, t, J=5.2 Hz), 4.20 (4H, br), 4.47 (2H, t, J=5.2 Hz), 5.69 (2H, s), 6.36 (2H, d, J=14.3 Hz), 7.19 (1H, s), 7.25 (2H, t, J=7.4 Hz), 7.41 (2H, t, J=7.7 Hz), 7.46 (2H, d, J=8.0 Hz), 7.60 (2H, d, J=7.4 Hz), 7.74 (1H, s), 8.09 (1H, s), 8.76 (2H, d, J=14.1 Hz). HR-ESI-MS m/z: 1077.4260 ($[M+2H-Na]^+$, Calcd for $C_{52}H_{69}N_8O_{11}S_3$: 1077.4242).

Analytical HPLC was performed on a reverse phase column (Waters symmetry C18 (3.5 μm particle size, 4.6 mm inner diameter×75 mm length), using eluent A (acetonitrile, 10% (0 min) to 90% (15 min)) and eluent B (10 mM ammonium formate buffer (pH 7.3)) at flow rate 1.0 mL/min at 40°C, fitted on Shimadzu LC-20AD pumps, SPD-M20A detectors, CTO-20A column oven, and LCMS solution system.

Optical Properties and Quantum Efficiency of Fluorescence Optical properties of dyes were examined in methanol using a Beckmann DU 640 UV-VIS spectrophotometer and JASCO FP-6600 fluorescence spectrophotometer. The slit width was 5 nm for excitation and 10 nm for emission. The fluorescence measurement was performed at 25°C.

For determination of the quantum efficiency of fluorescence (Φ_{fl}), indocyanine green (ICG) in methanol (Φ_{fl}=0.04) was used as a standard.[20] Values were calculated according to the following equation.

$$\Phi_x / \Phi_{st} = [A_{st} / A_x][D_x / D_{st}]$$

st: standard, x: sample. A: absorbance at the excitation wavelength. D: area under the fluorescence spectra on an energy scale.

Hydrophobicity Index (R_m) Value Rm values were determined according to the literature procedure.[21] In brief,

solution of test compounds were applied to the reversed-phase thin layer chromatography plate and developed in saturated chambers with mobile phase (10% 5 mM sodium phosphate buffer, pH 7.4 and 90% methanol). The separated spots were identified under visible light. The retention factor (R_f) values were obtained from the RP-TLC system and R_m values were calculated by the expression: R_m=Log ($1/R_f$−1).

***In Vitro* Fluorescence Assay of SUIT-2/HRE-Luc Cells Incubated under Different Oxygen Conditions** SUIT-2/HRE-Luc cells[18] were maintained at 37°C in 5% FCS-Dulbecco's-modified Eagle's medium (Nacalai Tesque, Kyoto, Japan) supplemented with penicillin (100 units/mL) and streptomycin (100 μg/mL). Hypoxic cell cultures were performed in 5% CO_2/0.1% O_2 in a INVIVO$_2$ 400 hypoxia workstation (Ruskinn Technology, Ltd., Bridgend, U.K.).

SUIT-2/HRE-Luc cells (2×10^5 cells/well) were seeded in a six-well plate and preincubated under normoxic (21% O_2) or hypoxic (0.1% O_2) conditions for 4 h, followed by incubation with 0.2, 1, or 5 μM of GPU-311 and 0.1% dimethyl sulfoxide (DMSO) for 30 min. Then, after the medium was changed, the cells were exposed to post-incubation for 1 h in fresh medium for releasing the unbound GPU-311 from the cells, washed with PBS, and suspended in 200 μL of radio-immunoprecipitation assay (RIPA) buffer. To evaluate cellular uptake including unbound probe, the cells were washed and lysed immediately after the probe treatment without post-incubation. Fluorescent intensity and NIR imaging were obtained using Infinite® F500 microplate reader (Tecan, Männedorf, Switzerland) and IVIS®-SPECTRUM (Caliper Life Sciences, Alameda, CA, U.S.A.), respectively. The amount of GPU-311 in the cells was calculated by using intensity–concentration curve. The excitation/emission wavelengths of filters were 740 nm/780 nm for the measurement of fluorescent intensity and 710 nm/800 nm for the fluorescent imaging, respectively. Statistical analysis was carried out with a Student's *t*-test. Values of $p<0.05$ were considered statistically significant.

***In Vivo* Fluorescence Imaging of SUIT-2/HRE-Luc Xenografts by GPU-311 and Analysis of T/B Ratio** All animal experiments were performed with the approval of Tokyo Institute of Technology and in accordance with the Ethical Guidelines for Animal Experimentation of Tokyo Institute of Technology. Male Balb/c nu/nu were purchased from Oriental Yeast Co., Ltd. All mice underwent experiments at 6—10 weeks of age. Low fluorescence background diet was fed to experimental mice. SUIT-2/HRE-Luc cells suspended in PBS (1.0×10^6 cells/20 μL) were mixed with an equal volume of Geltrex (Invitrogen, Carlsbad, CA, U.S.A.) and injected into both forelegs of 7-week-old male nude mice. Mice with subcutaneous tumors of 5—15 mm in diameter were used for experiments.

According to the method described previously,[19] we performed *in vivo* imaging and analysis of T/B ratio. In brief, 10 nmol of GPU-311 in 100 μL of PBS (pH 8.0) containing 0.2% DMSO were injected into tumor-bearing mice intravenously. *In vivo* fluorescence images were acquired at the indicated times with IVIS®-SPECTRUM (excitation filter: 710 nm, emission filter: 800 nm). Photon flux/sec in the same area (region of interest: ROI) of the tumors and the muscle in the lower limbs were counted at the indicated time after GPU-311 injection. Each photon flux/sec was normalized by subtracting photon flux/sec in the corresponding ROI of background. The relative fluorescence intensity of the tumor to the muscle (T/B ratio) was calculated by dividing the normalized values in tumors by ones in the muscle.

HIF-1-active hypoxic tumor was detected by bioluminescent bioimaging. For *in vivo* photon counting to assess bioluminescence, tumor-bearing mice were intraperitoneally injected with 200 μL of D-luciferin solution (10 mg/mL in PBS, Promega, Madison, WI, U.S.A.) and examined for bioluminescence images at 20 min after the injection of D-luciferin by IVIS®-SPECTRUM.

Acknowledgements This research was supported in part by a Grant from The Saijiro Endo Memorial Foundation for Science & Technology (to K.O.), a Grant-in-Aid for Young Scientists (B) (22790042 to K.O.), a Grant-in-Aid for Scientific Research on Priority Areas (20011009 to H.N.) from the Japan Society for the Promotion of Science, and a Grant-in-Aid for Scientific Research on Innovative Areas "Integrative Research on Cancer Microenvironment Network" (22112009 to S.K.K.) from the Ministry of Education, Culture, Sports, Science and Technology of Japan. We also thank Mr. Ryosuke Sakai, Mr. Takahiro Ueno, and Ms. Emi Inaba for their technical assistance.

References

1) Wilson W. R., Hay M. P., *Nat. Rev. Cancer*, **11**, 393—410 (2011).
2) Vaupel P., *Exp. Oncol.*, **32**, 125—127 (2010).
3) Osinsky S., Zavelevich M., Vaupel P., *Exp. Oncol.*, **31**, 80—86 (2009).
4) Kizaka-Kondoh S., Konse-Nagasawa H., *Cancer Sci.*, **100**, 1366—1373 (2009).
5) Sun X., Niu G., Chan N., Shen B., Chen X., *Mol. Imaging Biol.*, **13**, 399—410 (2011).
6) Chitneni S. K., Palmer G. M., Zalutsky M. R., Dewhirst M. W., *J. Nucl. Med.*, **52**, 165—168 (2011).
7) Astner S. T., Shi K., Vaupel P., Molls M., *Exp. Oncol.*, **32**, 149—152 (2010).
8) Pham W., Medarova Z., Moore A., *Bioconjugate Chem.*, **16**, 735—740 (2005).
9) Lewis J. S., Achilefu S., Garbow J. R., Laforest R., Welch M. J., *Eur. J. Cancer*, **38**, 2173—2188 (2002).
10) Okuda K., Yuossif B. G. M., Ueno T., Kadonosono T., Kizaka-Kondoh S., Nagasawa H., "The 2010 World Molecular Imaging Congress," Kyoto, Japan, September 8—11, 2010.
11) Flanagan Jr. J. H., Khan S. H., Menchen S., Soper S. A., Hammer R. P., *Bioconjugate Chem.*, **8**, 751—756 (1997).
12) Lee H., Mason J. C., Achilefu S., *J. Org. Chem.*, **71**, 7862—7865 (2006).
13) Song F., Peng X., Lu E., Zhang R., Chen X., Song B., *J. Photochem. Photobiol., A*, **168**, 53–57 (2004).
14) Zhao N., Roesler S., Kissel T., *Int. J. Pharm.*, **411**, 197—205 (2011).
15) Kolb H. C., Sharpless K. B., *Drug Discov. Today*, **8**, 1128—1137 (2003).
16) Yap S., Woodman O. L., Crack P. J., Williams S. J., *Bioorg. Med. Chem. Lett.*, **21**, 5102—5106 (2011).
17) Zhang L., Sun L., Cui Z., Gottlieb R. L., Zhang B., *Bioconjugate Chem.*, **12**, 939—948 (2001).
18) Kizaka-Kondoh S., Itasaka S., Zeng L., Tanaka S., Zhao T., Takahashi Y., Shibuya K., Hirota K., Semenza G. L., Hiraoka M., *Clin. Cancer Res.*, **15**, 3433—3441 (2009).
19) Kuchimaru T., Kadonosono T., Tanaka S., Ushiki T., Hiraoka M., Kizaka-Kondoh S., *PLoS ONE*, **5**, e15736 (2010).
20) Soper S. A., Mattingly Q. L., *J. Am. Chem. Soc.*, **116**, 3744—3752 (1994).
21) Cardoso M. G., Nelson D. L., Tavares do Amaral A., Donizete dos Santos C., Pereira A. A., Barenche de Oliveira A. C., *Int. J. Mol. Sci.*, **3**, 755—763 (2002).